Detection of lung cancer using Ten Convolutional Neural Network Models

Mr.R.Kishore, Dr.R.Suresh babu
Department of ECE,
Kamaraj College of engineering and technology,
Anna University, Chennai, India.
kishoreresearchscholar@gmail.com,hodece@kamarajengg.edu.in

Abstract

Lung cancer accounts for more than 1.5 million deaths worldwide, and it corresponded to 26% of all deaths due to cancer in 2017. However, lung computer aided detection (CAD) scheme was developed to identify this syndrome at a beginning phase for increasing survival rates. Initially, the 1018 chests computed tomography (CT) examinations and medical annotations from the LIDC/IDRI were processed. So, the lung CAD scheme using ten Convolutional Neural Network (CNN) Models was developed to examine a thoracic CT image slice. This work investigates a recent study of ten CNN Models, trained on an image net dataset, converted into feature extractors and applied to the LIDC/IDRI nodule images. Following this, each set of deep features was submitted to 10 fold cross validations with 3 classification techniques. Finally, the parameter of each cross validated result was computed and compared. Results have demonstrated for our excellent model capability which yields 91.79% accuracy and 92.24% sensitivity (false positive is 0.24). Based on these results, our lung CAD scheme was developed to assist radiologists in a better manner and ten CNN models was proved to extort representative features from lung nodule CT images.

Keywords: *Convolutional Neural Network, deep feature, classification, sensitivity, accuracy*

1. Introduction

1.1 General

Lung cancer is a single hazardous syndrome, which might present in small as well as non small cell. It is a prime cause for both genders in many countries. Early detection has high endurance rate. But, it is usually noticed late due to the lack of symptom in its early phases. So, it's endurance prolongs to fall. Hence, 7.6% males as well as 11.3% females are net survival predicted during 2013-2017 and it is indicated in Table 1.1 Also more than 50% lung patients are noticed at a later phase in which five-year endurance rate is only 4%; consequently, this is regarded as a hostile disease due to its significant morbidity and mortality. According to a World Health Organization survey, lung cancer has been the largest cause of cancer deaths among male patients, while in female patients, lung cancer deaths rank second only to breast cancer [3, 4]. Therefore, early detection is significant for lung cancer diagnosis, which can greatly increase a lung cancer patient's chance of survival.

Computed tomography (CT) is a powerful system for noticing premature phase lung cancer, by identifying malignant lung nodules [5]. However, the intensity variation in CT scans images and anatomical structure misjudgments by doctors and radiologists may cause difficulty in marking the cancerous cell. So, it is a quite exhausting task for radiologists to carefully examine each CT image, of which there was a large amount. Meanwhile, the diagnosis is affected by the limitation of the radiologists capability, which increases the possibility of mis-diagnosis. To evade the radiologists subjectivity factor and reduce their burden, computer aided

Table 1.1 Lung cancer standardised one, five and ten year net survival (2013-2017)

Sex	Years after diagnosis	Number of cases	Net surivival (%)
Female	one year	85,270	44.5
Male	one year	98,357	37.1
Persons	one year	183,627	40.6
Female	five years	85,270.0	19.0
Male	five years	98,357.0	13.8
Persons	five years	183,627.0	16.2
Female	ten years	134,006.0	11.3
Male	ten years	157,189.0	7.6
Persons	ten years	291,195.0	9.5

detection can find the lung nodule location and predict lung cancer risk, can be utilized to support radiologists with the speed and accuracy of diagnosis [6,7].

A tiny cell presented in parenchyma region has an abnormal growth. To aid the specialist with the information regarding cells, computer-aided detection (CAD) [31] system was expanded. It was designed to identify the nodule sized between 3 and 30 mm. Before deep learning methods emerge, it was usually associated by two steps: first, handcrafted feature extortion [9,10]. Second, support vector machine (SVM) classifier [11] or random forest [12] technique was employed to classify these featured nodules. Attributes utilizing histogram [13], local binary patterns (LBP) [14], and wavelets [15] were utilized for feature extortion. Without these automatic feature extortion methods, they can also extort handcrafted features in terms of geometry [16], appearance [17], or texture [18].

Segmentation is a crucial phase in many purposes involving CAD. During modern years, a lot of segmentation procedures are proposed, which can be grouped as thresholding technique [7,8], morphological technique [9], deformable model [10], clustering method [11–13], graph cut method [14,15], Markov random field, region growing [16], watershed, neural networks, fuzzy logic [32], active contours [35] and histogram based segmentation [18].

For example, Gurcan et al. [8] utilized weighted k-means clustering to segment lung area and classified them by utilizing a rule-based classifier scheme to diminish false positive (FP) objects per slice. Their work can attain 84% sensitivity (5.48 FP objects per slice). Elmar et al. [11] computed several masks to eliminate the background and surrounding tissue and utilized SVM to categorize the regions of interest with a sensitivity of 84.93%, specificity of 80.92%. In 2006, Geoffrey and his team [19] suggested a quick training procedure for deep belief net design.

Recently, by the expansion of CNN models, more and more teams utilize CNNs to do medical image diagnosis tasks. Rotem et al. [26] utilized Alexnet to extort valuable features of the input data and attained a sensitivity of 78.9% (20 false positives per scan (FPs/scan)). Shuo et al. [27] presented multi-view convolutional neural networks for lung nodule segmentation. The architecture may acquire a set of nodule feature from axial, coronal, and sagittal views in CT scans, so it has attained a sensitivity of 83.72% (20.71 FPs/scan).

In this work, a lung cancer in early stage needs to be identified using ten CNN models which was based on Imagenet database.

1.2 Related works

Aggarwal, Furquan and Kalra [36] proposed a system that provides classification between nodules and normal lung anatomy structure. The method extracts geometrical, statistical and gray level characteristics by utilizing LDA and optimal threshold approach. It has 84% accuracy, 97.14% sensitivity and 53.33% specificity. Although the method notices the cancerous nodule, its specificity is still unacceptable. No machine learning methods are utilized in classification step and simple segmentation techniques are utilized. Therefore, the combination of any of its steps in our new approach does not provide a probability of improvement. Jin Zhang and Jin [37] utilized convolution neural network as a classifier in his CAD system to detect the lung cancer. The system has 84.6% accuracy, 82.5% sensitivity and 86.7% specificity. The advantage of this model is that it utilizes a circular filter in the Region of interest (ROI) re-extraction phase, which reduces the cost of training and recognition steps. Although, implementation cost is reduced, it has still unsatisfactory accuracy. Sangamithra and Govindaraju [38] utilizes K mean unsupervised learning algorithm by using pixel dataset according to certain characteristics. For classification, this model implements back propagation network. Features like entropy, correlation, homogeneity, PSNR, SSIM are extorted. The system has 90.7% accuracy. During image pre- processing phase, median filter [33] [34] has utilized which can be helpful for our new approach. Roy, Sirohi, and Patle [39] developed a system to detect lung cancer nodule using fuzzy interference system and active contour model. It utilizes gray transformation. Cancer classification is performed using fuzzy inference method. Features like area, mean, entropy, correlation, major axis length, minor axis length are extorted to train the classifier. Overall, system accuracy is 94.12%. Counting its limitation it does not categorize cancer as benign or malignant. Ignatius and Joseph [40] developed a system utilizing watershed

segmentation. In pre-processing it uses a Gabor filter to enhance the image quality. It compares the accuracy with neural fuzzy model and region growing method. Accuracy of the proposed is 90.1%, which is comparatively higher than the model with segmentation using neural fuzzy model and region growing method. The advantage of this model is that it utilizes marker controlled watershed segmentation which solves over segmentation problem. As a limitation it does not classify cancer and has higher accuracy but still not satisfactory. Some changes and contribution of this model has a probability of increasing the accuracy to a satisfactory level. Gonzalez and Ponomaryvo [41] proposed a system that classifies lung cancer as benign or malignant. The system utilizes the priori information and HousefieldUnit(HU) to calculate Region of Interest (ROI). Shape features like area, eccentricity, circularity, fractal dimension and textural features like mean, variance, energy, entropy, contrast, and smoothness is extorted to train and categorize support vector mechanism to recognize whether the nodule is benign or malignant.

2.1 Methodology

Fig 2.1 illustrates a processing of CT image using LIDC/IDRI database and deep feature extractor. This figure is organized into three sections, database processing, implementation approach and its evaluation. Each section is characterized by a sequence of steps. Each step was simplified in the block diagram.

The database processing (utilized in this work to represent the lung nodule malignancy classification task) can be divided into two phases: processing the medical annotations and reducing the problem. The first phase requires 5 steps. In the first step, the 1018 LIDC/IDRI database examinations, which are initially an unordered sequence of DICOM files, are sorted and then converted into a single three-dimensional array. Also, there is an XML file for each CT examination, containing the medical annotations of 4 experienced radiologists. Among other information, each one of these physicians also marked the external contour coordinates and malignancy level of each nodule detected.

Based on this information, it is also possible to compute the centroid of the nodule in question and its largest radius (the largest Euclidean distance between the centroid and a contour point). Fig 2.2 illustrates the processing of LIDC/IDRI medical annotations using XML file. However, it is common and even expected, to have nodules detected, segmented and categorized by more than one radiologist. In addition, allowing two or more samples with a high degree of similarity to be at the same time in the training and test sets reduces the database representativeness and, consequently, the reliability of the classification process. In the second step, a strategy for merging these redundant annotations is proposed. First, the Euclidean distances between the centroids of all the annotations of a given examination are computed.

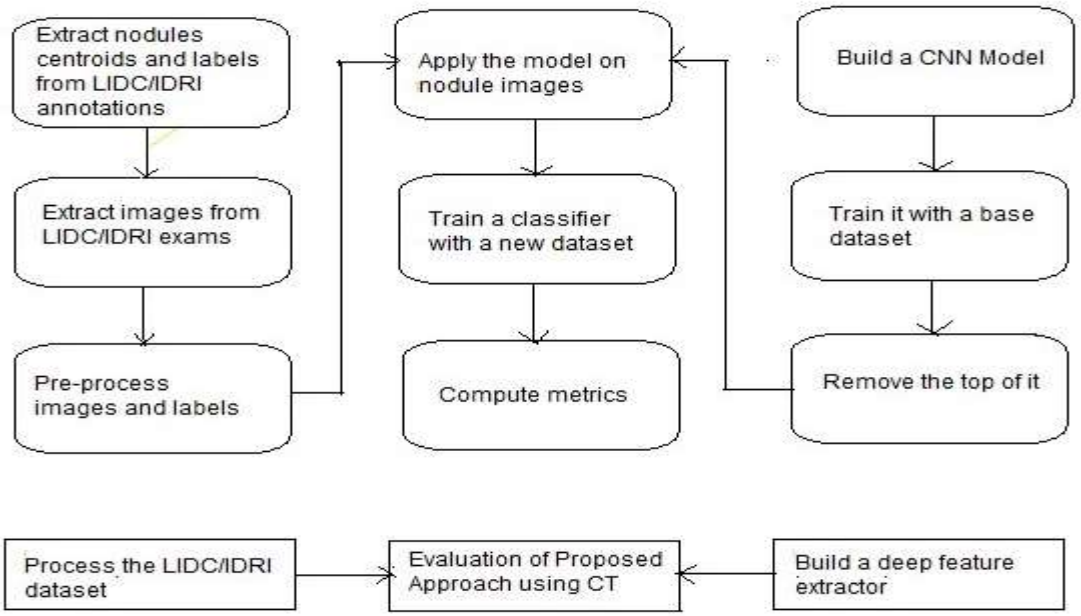

Fig 2.1 Processing of CT image using LIDC/IDRI database and deep feature extractor

2.1.1 Processing the medical annotations

Then, the centroids that are distant by a smaller value than 80% of their respective radius have their annotations combined. This process of merging the annotations consists of computing the midpoint between the centroids and the median of their malignancy levels. This process of handling redundant annotations is illustrated in Fig 2.3

In a third step, after ensuring that there is only one annotation per nodule, the centroids are located in the three-dimensional matrix which was produced as the first step of this part. Then, the 16 voxels surrounding the centroids are copied and stored in a list. This process of extorting the volumes of interest is illustrated in Fig 2.4

In the fourth step, each one of these volumes of interest is sub-sampled and transformed into a 3-channel image. An illustration of this transformation is shown in Fig 2.5 In the fifth and last step of this stage, the set of nodule images is submitted to a sequence of treatments: centralization, normalization and formation. During the centralization treatment, the average value of each channel of each image is computed and, later, subtracted from its elements. In the normalization treatment, these channels are normalized by their respective standard deviations. Finally, the images are resized in height and width to meet the input resolutions specified by each architecture used in this work.

\

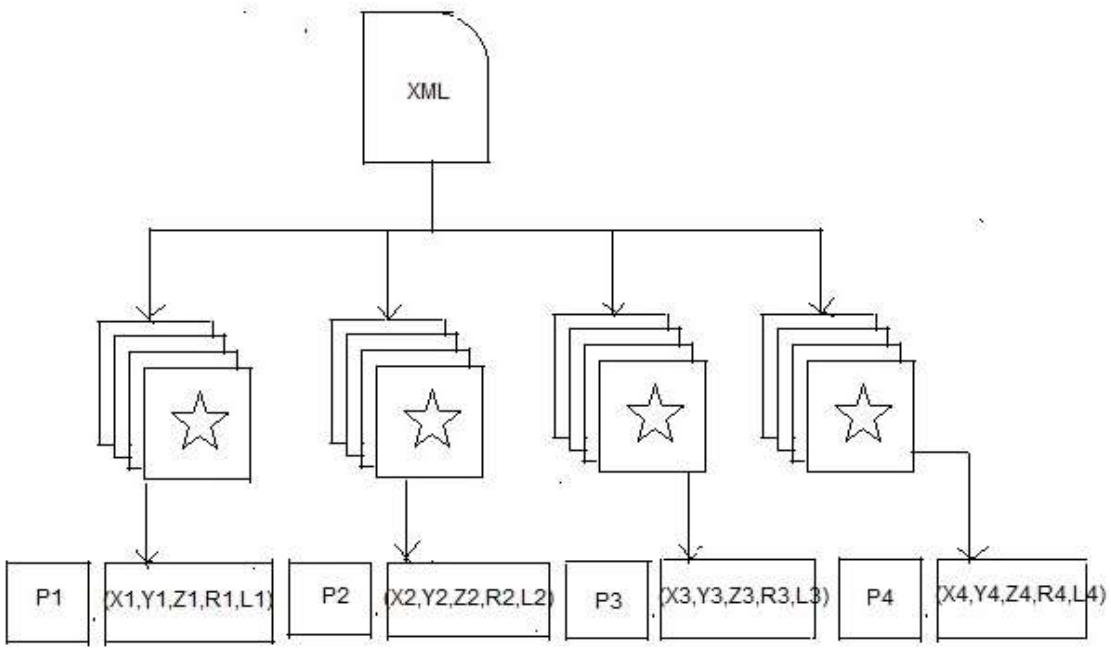

Fig 2.2 Processing of LIDC/IDRI medical annotations using XML file

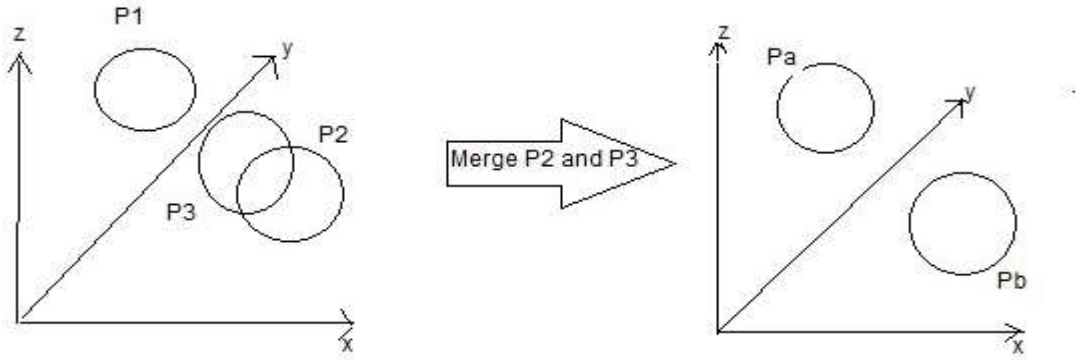

Fig 2.3 Reduction of Problem Space

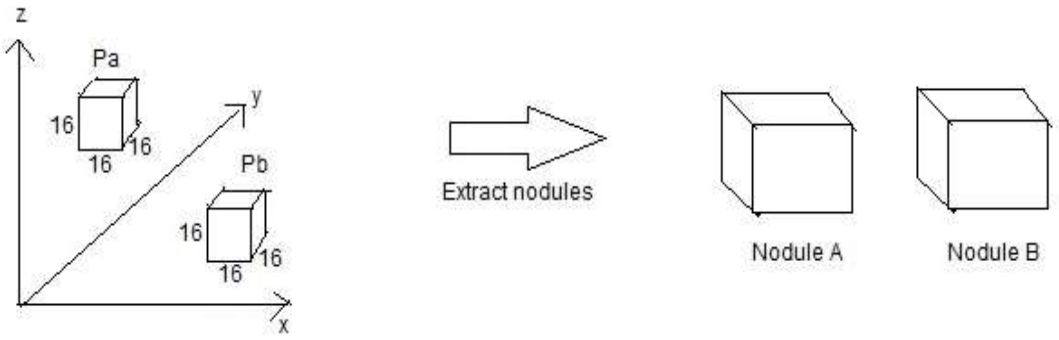

Fig 2.4 Extraction Process for the Volumes of Interest

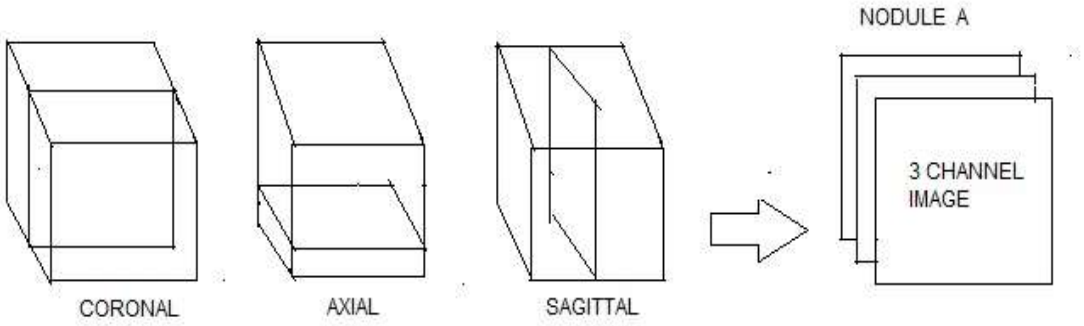

Fig 2.5 Converting an extracted volume of interest into a three channel image

2.1.2 Problem reduction

During the LIDC/IDRI database design procedure, radiologists were instructed to assign a level of malignancy between 1 and 5 for each node noticed. However, the vast majority of studies in the literature (using the LIDC/IDRI database) restrict the task of lung nodule malignancy classification to a binary classification problem. Therefore, in order to maintain a methodological standard among the comparison works, a reduction procedure was applied. This procedure combines and labels levels 1 and 2 as non-malignant nodules, while levels 4 and 5 are combined and labeled as malignant nodules. The distribution of the number of samples per class before and after the reduction process is illustrated in Fig 2.6

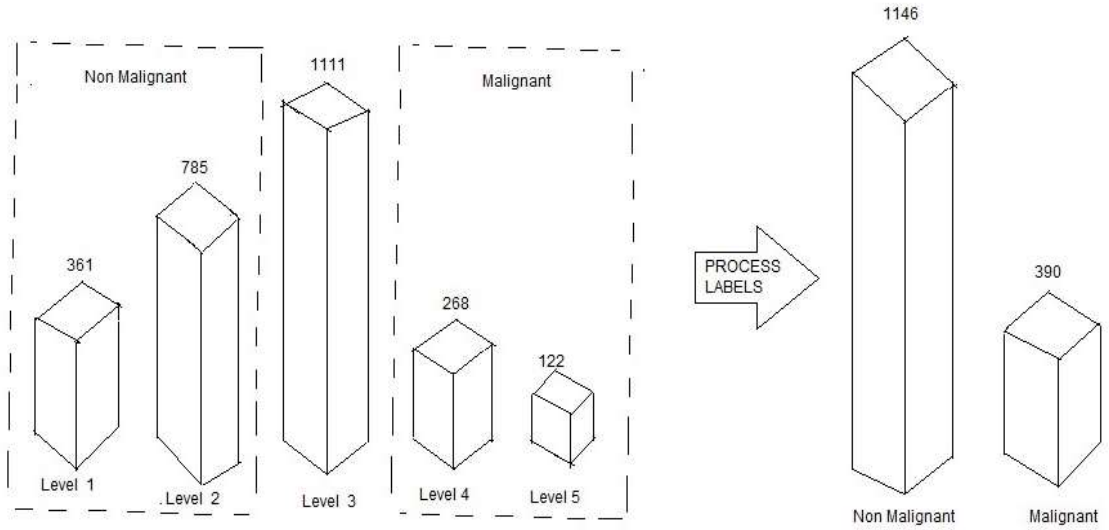

Fig 2.6 Distribution of the number of samples per class before and after the reduction process

2.2 Existing computer aided detection scheme

Image Acquisition

CT images are obtained by utilizing LIDC-IDRI dataset. These images are having a resolution of 512 × 512 pixels, where the number of slices may range from 65 to 764.

Image Pre-processing

In this step, we begin image improvement and utilize three methods which was listed here: Gabor, auto-enhance, Fast Fourier transforms.

Image Segmentation

Image segmentation plays a vital module involved during lung region extortion. In particular, various existing mechanisms depend upon an adaptive threshold segmentation scheme. However, a threshold technique has drawn a lot of attention during the past two decades.

Feature Extortion

The features extortion phase is an important technique from the desired portion of an image. It is an essential stage, which represents the final results to determine normality or abnormality of an image. These features act as the basis for classification step. Only these features were considered

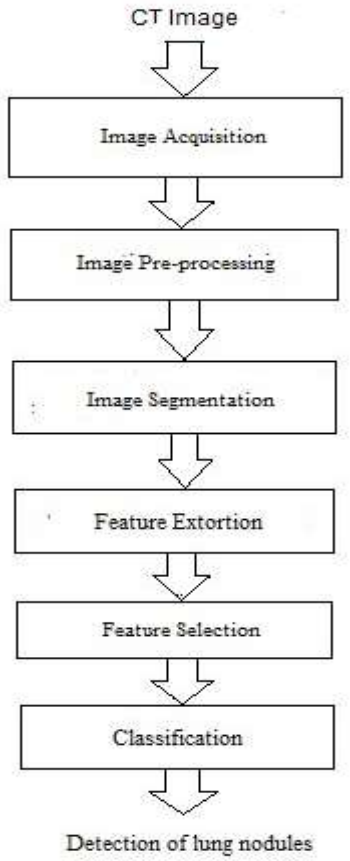

Fig 2.7 Existing computer aided detection scheme

to be extorted; average intensity, area, perimeter and eccentricity. The features are defined as follows:

1) Area: it is a scalar value that gives the actual number of overall nodule pixel. It is obtained by the summation of areas of pixel in the image that is registered as 1 in the binary image obtained.

2) Perimeter: It is a scalar value that gives the actual number of the outline of the nodule pixel. It is obtained by the summation of the interconnected outline of the registered pixel in the binary image.

3) Eccentricity: This metric value is 1 for circular and is <1 for any other shape.

Classification

Lung nodules are nominal growth in the lung, which was used to measure between 5mm to 25mm. Feature extortion has used to extort the features from the nodule by which we can identify the phases of lung cancer.

2.3 CNN Architecture

2.3.1 Model construction and initialization

Over the last few years, especially since 2012, the performance in object recognition tasks has drastically increased by using various CNN models. However, it is not feasible to assess all architectures elaborated by the scientific community, 10 reputable models were selected to represent the CNN class. The computational graphs representing such models (VGG16, VGG19, Alex net, squeeze net, goggle net, inceptionv3, densenet201, mobilenetv2, resnet18 and Xception) were implemented and initialized.

In Fig 2.8, each CNN model contains an input layer, number of hidden layers and an output layer. The knowledge of these networks is utilized to classify the images effectively.

2.3.2 Model training

The second phase is the training of the 10 models with the reference database from which the knowledge is transferred. Furthermore, since all 10 models were elaborated with the objective of solving the problem represented by an image net database, which contains 1.2 million non-medical images and divided into 1000 categories, deep learning methods are utilized by each of them.

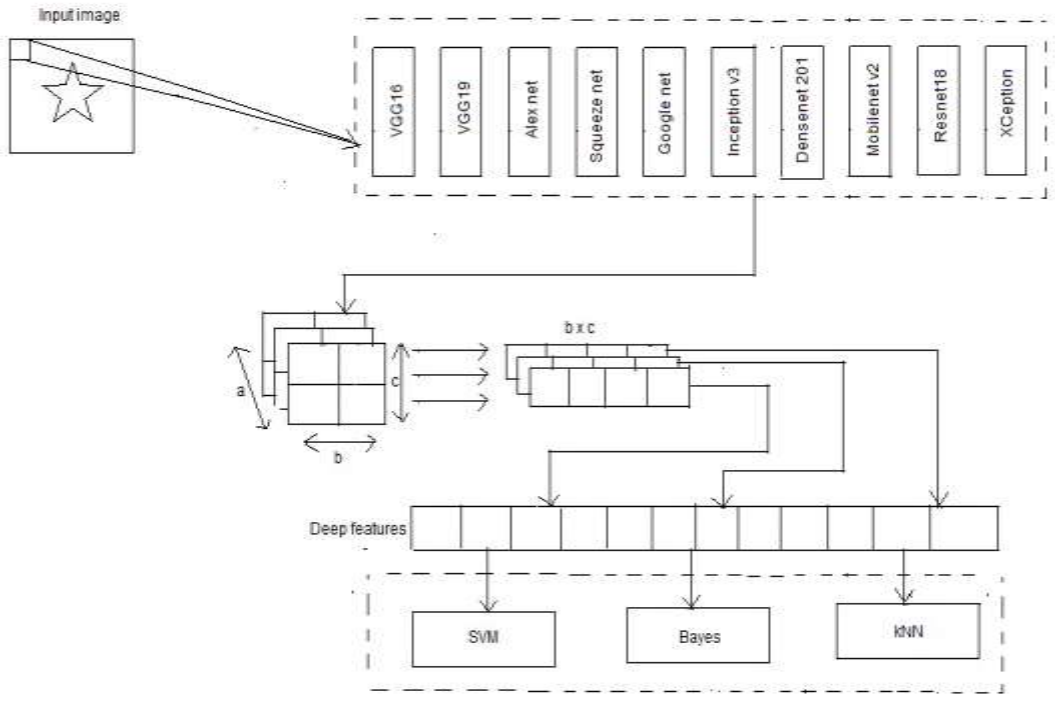

Fig 2.8 Image passing to CNN Model

Table 2.1 Specification of each CNN Model

Network	Depth	Size	Parameters (Million)	Image Input Size
Alexnet	8	227 MB	61.0	227-by-227
Vgg16	16	515 MB	138	224-by-224
Vgg19	19	535 MB	144	224-by-224
Squeezenet	18	4.6 MB	1.24	227 by 227
Googlenet	22	27 MB	7.0	224-by-224
Inceptionv3	48	89 MB	23.9	299-by-299
Mobilenetv2	53	13 MB	3.5	224-by-224
Densenet201	201	77 MB	20.0	224-by-224
Resnet18	18	44 MB	11.7	224-by-224
Xception	71	85 MB	22.9	299-by-299

2.3.3 Converting CNN into feature extractor

In the third and last step of this part (as referred in fig 2.9), CNN model trained using reference dataset are converted into feature extorter. However, to accomplish this, it is necessary to understand four transformations which were performed using neural network. First, a CNN input image is initially submitted to a nonlinear transformation sequence, which are defined according to the architecture used. This process converts the input image into a set of small arrays. Subsequently, each of these matrices is resized to a one dimensional vector. Then, this set of vectors is concatenated, thus forming a single vector. Each vector, in turn, can be interpreted as the features extorted by CNN. Finally, each deep feature was submitted to three classifiers. In general, it resembles the processing performed using cross validated datasets.

3 Proposed Approach Evaluation

3.1 Extracting features from LIDC/IDRI database

First, the CNN model transferred into feature extorts are applied to the LIDC/IDRI database after preprocessing performed in the first part of this section. As most classifiers process same image more than once during their training, it is preferable to transfer the whole target database into 10 new feature sets (one for CNN model) before training. This avoids the computational cost of performing the extortion task more than once, thus reducing the time consumed during the evaluation process.

3.2 Malignancy classification

To evaluate how representative is the features extorted, each 10 datasets generated previously is classified using 3 consolidated families of classification techniques: naive Bayes, support vector machine (SVM) and nearest neighbors (KNN). In the naive Bayes, a Gaussian distribution is utilized as a probability density function. In a KNN classifier, a number of neighbors (hyper-parameter) were chosen through a grid search, which tests an odd value between 1 and 11. While for the SVM classifier, a hyper-parameter was chosen through a random search with 20 iterations over each fold of a 10-fold cross-validation process, which is illustrated in Fig 3.1

3.3 Evaluation metrics

True positive (TP) is a quantity of malignant nodules which are correctly classified; true negative (TN) is a quantity of non-malignant nodules which are correctly classified; false positive (FP) is a quantity of non-malignant nodules which are wrongly classified; and false negative (FN) is a quantity of malignant nodules which are wrongly classified. Based on these values, the evaluation metrics ACC, SEN, SPEC can be mathematically described by the following equations:

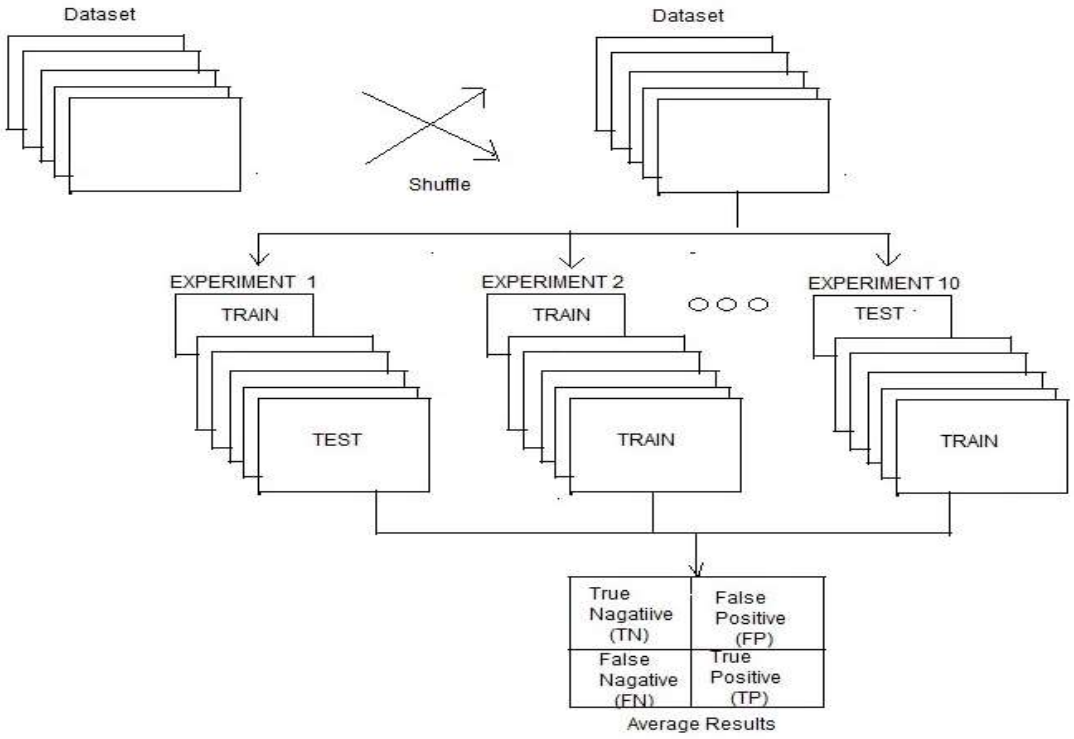

Fig 3.1 Cross validation step in a shuffled data set

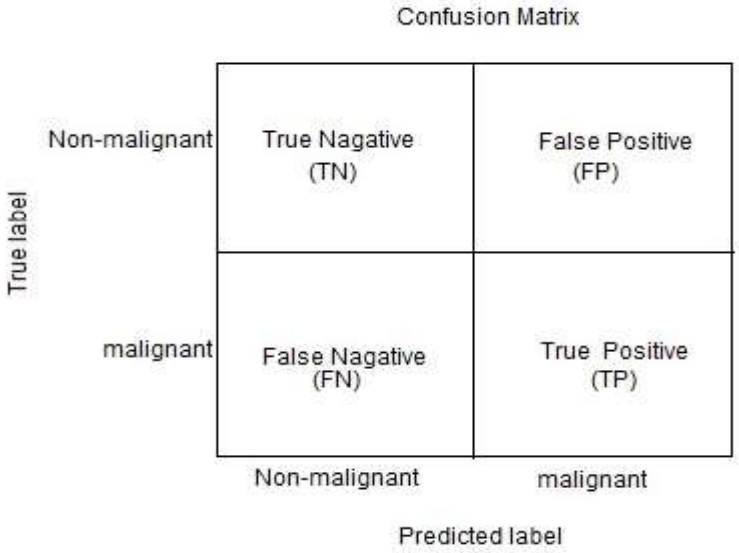

Fig 3.2 Confusion matrix

ACC = (TP+TN) / (TP + TN + FP + FN) ⟶ (1)

SEN = TP / (TP+FN) ⟶ (2)

SPE = TN / (TN+FP) ⟶ (3)

Moreover, to compute the AUC evaluation metric, two steps are required. In the first, the validated samples are divided into two groups, the non-malignant nodules and the malignant ones. Next, each of these sets is submitted to a prediction process of a given classifier and the correct class prediction scores are used to compute a histogram. Then, these two histograms are plotted into a graph as illustrated in Fig 3.3

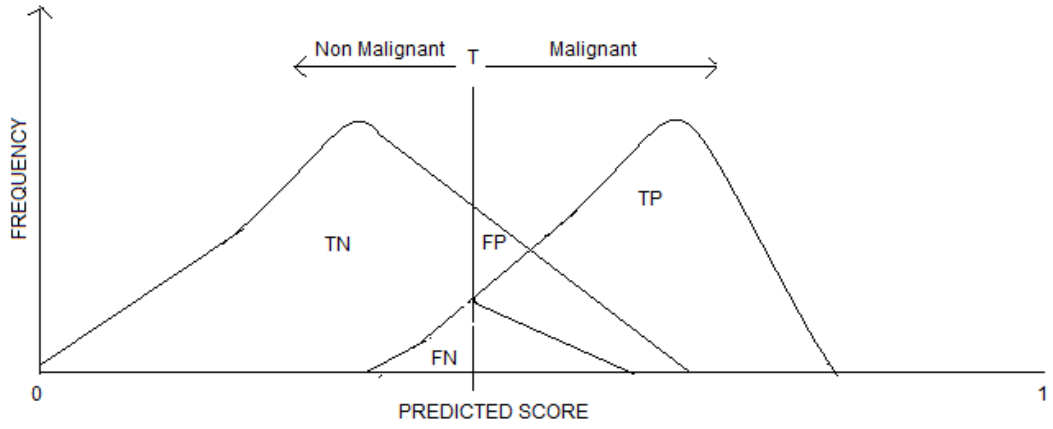

Fig 3.3 Prediction probability histogram of a binary problem, where TP, TN, FP and FN are true positive, true negative, false positive and false negative, respectively. T is the threshold between what is classified as class 0 and class 1

This graph shows that as the parameter T varies, the relation between the values of TP, TN, FP and FN also changes and consequently, the same happens with the sensitivity and specificity metric, which is represented in the equation (2) and (3).

Table 3.1

		Accuracy(%)	Sensitivity	Specificity	False Positive
Squeezenet	SVM	85.212	0.92	0.883	0.42
	Naïve bayes	83.514	0.94	0.852	0.49
	kNN	87.207	0.80	0.901	0.16
Alexnet	SVM	98.79	0.940	0.949	0.06
	Naïve bayes	99.10	0.961	0.959	0.04
	kNN	99.79	0.980	0.969	0.03
VGG16	SVM	86.53	0.872	0.885	0.38
	Naïve bayes	87.60	0.882	0.875	0.23
	kNN	88.60	0.885	0.820	0.03
VGG19	SVM	88.90	0.882	0.885	0.40
	Naïve bayes	89.51	0.872	0.860	0.25
	kNN	90.05	0.921	0.905	0.06
Inceptionv3	SVM	89.87	0.891	0.870	0.35
	Naïve bayes	90.87	0.882	0.860	0.30
	kNN	92.87	0.903	0.912	0.25
Mobilenetv2	SVM	93.3	0.973	0.963	0.32
	Naïve bayes	92	0.964	0.943	0.26
	kNN	90.3	0.983	0.954	0.20
Google net	SVM	99.79	0.980	0.999	0.03
	Naïve bayes	99.80	0.983	0.971	0.02
	kNN	99.90	0.986	0.941	0.01
Xception	SVM	89.28	0.895	0.890	0.38
	Naïve bayes	95.5	0.986	0.941	0.23
	kNN	96.5	0.895	0.890	0.10
Resnet18	SVM	81.41	0.873	0.854	0.46
	Naïve bayes	95.5	0.986	0.941	0.22
	kNN	96.5	0.895	0.890	0.12
Densenet201	SVM	88.82	0.885	0.878	0.42
	Naïve bayes	81.41	0.873	0.854	0.23
	kNN	95.5	0.986	0.941	0.14

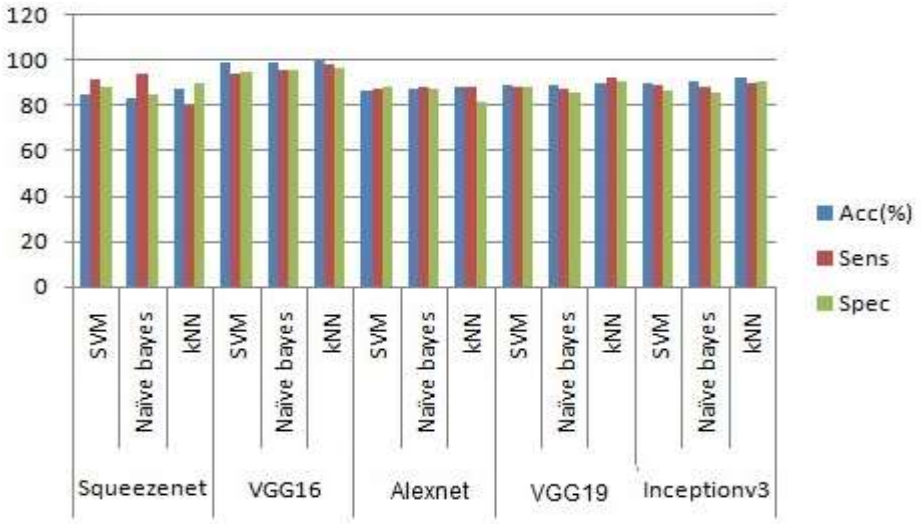

Fig 3.3 Top five combination (Acc, Sen, Spe)

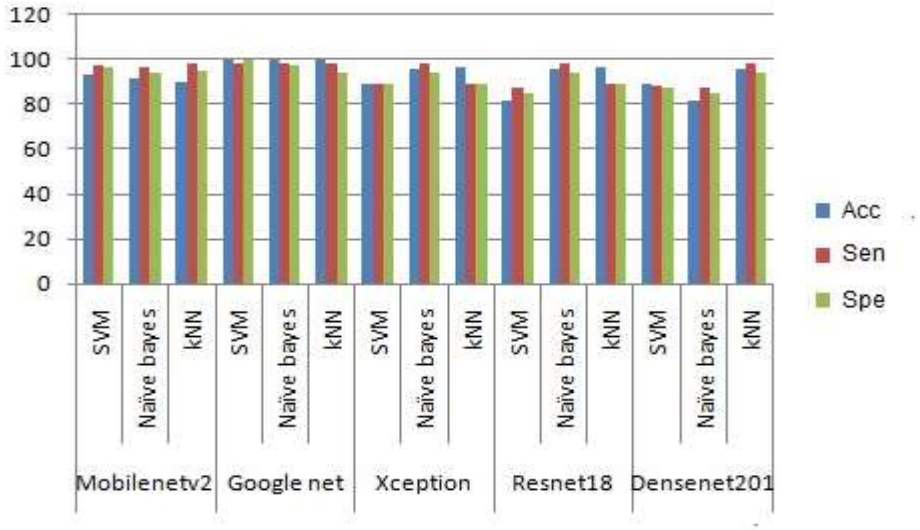

Fig 3.4 Top five combination (Acc, Sen, Spe)

4. Discussion

In this study, a novel pulmonary nodule recognition CAD scheme using 10 CNN model is proposed. Compared to published CAD systems that are evaluated on the publicly available

LIDC-IDRI dataset, our proposed CAD scheme achieves comparable or better performance, indicating the potential of using pre-trained CNN on Image net instead of using engineered features and classification as the FP reduction stage. It suggests that the possibility of learning features from large natural image training dataset allows the network to learn classifying objects with a high degree of variation, which is suitable for the problem of pulmonary nodule detection.

For 10 CNN models, we used three classifiers (SVM, Naïve Bayes, kNN) for identifying lung cancer in an early phase.

Table 4.1

	Methods	Acc	Sen	FP/s
1	Sivakumar, S et al.	83.6%	82.1%	
2	Lu L et al.	84.8%	85.2%	3.13
3	Liu J-K et al.	84.1%	81.3%	4.5
4	Kumar D et al	75.0%	83.35%	0.39
5	A. Setio et al	80.1%	85.4%	4
6	Jiang H et al	80.06%	84%	4.7
7	Proposed 10 CNN Models	91.79%	92.24%	0.24

This preliminary work examines the effectiveness of using 10 CNN models to distinguish nodules and non-nodules. This study can be extended to various classification tasks and can be utilized hierarchically, with models trained to localize nodule candidates and quantify. Some reasons of classification success include the automatic extortion of features rather than an artificial calculation way. In practice, it is impossible to extort effective features without knowing the real meaning of nodule features by CNN. For that reason, we utilized a CNN model in our work for feature extortion. Also, the state-of-the-art 10 CNN models perform well in image classification tasks, however, limited by the size of image library, it is hard to train ten CNN models for nodule detection. For this reason, we utilized a fine-tuned CNN model in our work for feature extortion. It can be concluded that it will hold a good option for focal lesion classification.

5. Conclusion

Our proposed computer aided detection scheme using 10 CNN Models attained 91.79% accuracy and 92.24% sensitivity is better to recognize lung cancer in beginning phase for improving survival rates. It is a promising method for radiologists to recognize an abnormality by computed tomography images from LIDC-IDRI image set. By utilizing 10 CNN Models, false positive of the proposed CAD scheme have diminished to 0.24 which was lower than previous works

6. References

[1] *https://www.statisticshowto.com/receiver-operating-characteristic-roc-curve/*

[2] *https://acutecaretesting.org/en/articles/roc-curves-what-are-they-and-how-are-they-used*

[3] *Siegel RL, Miller KD and Jemal A, "Cancer statistics", CA Cancer J Clin, Vol. 65, No. 1, (**2015**) pp 5–29.*

[4] *Ma L, Wang DD, Zou B and Yan H, "An eigen-binding site based method for the analysis of anti-EGFR drug resistance in lung cancer treatment", IEEE/ACM Trans Comput Biol Bioinform, Vol. 14, No. 5, (**2017**), pp 1187–1194.*

[5] *Kaneko M, Eguchi K, Ohmatsu H, Kakinuma R, Naruke T,Suemasu K and Moriyama N, "Peripheral lung cancer: screening and detection with low-dose spiral CT versus radiography", Radiology, Vol. 201, No.3, (**1996**), pp 798–802.*

[6] *Jiang H, Ma H, Qian W et al., "An automatic detection system of lung nodule based on multi-group patch-based deep learning network", IEEE J Biomed Health Inform 22, (**2017**) , pp 1227–1237.*

[7] *Messay T, Hardie RC, Rogers SK, "A new computationally efficient CAD system for pulmonary nodule detection in CT imagery", Med Image Anal (**2010**), Vol. 14, No. 3, pp 390–406.*

[8] *Gurcan MN, Sahiner B, Petrick N, Chan HP, Kazerooni EA,Cascade PN, Hadjiiski L, "Lung nodule detection on thoracic computed tomography images: Preliminary evaluation of a computer aided diagnosis system", Med Phys (**2002**), Vol. 29, No.11, pp 2552–2558.*

[9] Aerts HJ, Velazquez ER, Leijenaar RT, Parmar C, Grossmann P, Carvalho S, Bussink J,Monshouwer R, Haibe-Kains B, Rietveld D, Hoebers F, "*Decoding tumour phenotype by noninvasive imaging using a quantitative radiomics approach",* Nat Commun (2014) Vol. 5, No. 4006.

[10] *Balagurunathan Y, Gu Y,Wang H, Kumar V, Grove O, Hawkins S, Kim J, Goldgof DB, Hall LO, Gatenby RA, Gillies RJ, "Reproducibility and prognosis of quantitative features extracted from CT images", Transl Oncol (**2014**), Vol. 7, No. 1, pp 72–87.*

[11] *Rendon-Gonzalez E, Ponomaryov V, "Automatic lung nodule segmentation and classification in CT images based on SVM", International Kharkiv Symposium on Physics and Engineering of Microwaves, Millimeter and Submillimeter Waves, IEEE(**2016**), pp 1–4.*

[12] *Lee S L A, Kouzani A Z and Hu E J, "A random forest for lung nodule identification", TENCON 2008 , IEEE Region 10 Conference, IEEE(**2008**), pp 1–5.*

[13] *Adetiba E, Olugbara OO, "Lung cancer prediction using neural network ensemble with histogram of oriented gradient genomic features", Scientific World Journal (**2015**), pp 1–17. https://doi.org/10.1155/2015/786013.*

[14] *Shan C, "Learning local binary patterns for gender classification on real-world face images", Pattern Recognit Lett (**2012**) , Vol. 33, No. 4, pp 431–437.*

[15] *Orozco HM, Villegas OOV, Sánchez VGC, Domínguez HJO, Alfaro MJN, "Automated system for lung nodules classification based on wavelet feature descriptor and support vector machine", Biomed Eng Online(**2015**), Vol. 14, No. 1, Issue 9.*

[16] *Tartar A, Akan A, Kilic N, "A novel approach to malignant-benign classification of pulmonary nodules by using ensemble learning classifiers", Conf Proc IEEE Eng Med Biol Soc (**2014**), pp 4651–4654.*

[17] *Kang G, Liu K, Hou B, Zhang N, "3D multi-view convolutional neural networks for lung nodule classification", PLoS One(**2017**), 12: e0188290*.

[18] *Han F, Wang H, Zhang G, Han H, Song B, Li L, Moore W, Lu H, Zhao H and Liang Z, "Texture feature analysis for computer-aided diagnosis on pulmonary nodules", Journal of Digital Imaging(**2015**), Vol. 28, No.1, pp 99–115.*

[19] *HintonGE,Osindero S, TehYW, "A fast learning algorithm for deep belief nets", Neural Comput(**2006**), https://doi.org/10.1162/neco.2006.18.7.1527*

[20] *Szegedy C, Liu W, Jia Y, Sermanet P, Reed S, Anguelov D, Erhan D, Vanhoucke V, Rabinovich A, "Going deeper with convolutions", Proc IEEE Comput Soc Conf Comput Vis Pattern Recognit(**2015**)*

[21] *Ren S, He K, Girshick R and Sun J, "Faster r-cnn: towards real-time object detection with region proposal networks", Adv Neural Inf Process Syst(**2015**), pp 91–99.*

[22] *Liang-Chieh C, Papandreou G, Kokkinos I, Murphy K and Yuille A, "Semantic image segmentation with deep convolutional nets and fully connected crfs", International Conference on Learning Representations (**2015**)*

[23] *Krizhevsky A, Sutskever I,Hinton GE, "Imagenet classification with deep convolutional neural networks",Adv Neural Inf Process Syst(2012), pp 1097–1105.*

[24] *Simonyan K, Zisserman A, "Very deep convolutional networks for large-scale image recognition", arXiv preprint arXiv:1409.1556(**2014**).*

[25] *He K, Zhang X, Ren S, Sun J, "Deep residual learning for image recognition", Proc IEEE Comput Soc Conf Comput Vis Pattern Recognit(**2016**), pp 770–778.*

[26] *Golan R, Jacob C, Denzinger J, "Lung nodule detection in CT images using deep convolutional neural networks", International Joint Conference on Neural Networks(**2016**), pp 243–250.*

[27] Wang S, Zhou M, Gevaert O, Tang Z, Dong D, Liu Z and Tian J, "A multi view deep convolutional neural networks for lung nodule segmentation", Conf Proc IEEE Eng Med Biol Soc(2017), pp 1752–1755.

[28] *Liu K, Kang G, "Multiview convolutional neural networks for lung nodule classification", Int J Imaging Syst Technol (**2017**), DOI:https://doi.org/10.1002/ima.22206.*

[29] *Huang X, Shan J, Vaidya V, "Lung nodule detection in CT using 3D convolutional neural networks". IEEE 14th International Symposium on Biomedical Imaging (**2017**) , pp 379–383.*

[30] *Gu Y, Lu X, Yang L, Zhang B, Yu D, Zhao Y, Gao L, Wu L and Zhou T, "Automatic lung nodule detection using a 3D deep convolutional neural network combined with a multi-scale prediction strategy in chest CTs", Comput. Biol. Med. 103(**2018**), pp 220–231.*

[31] *https://www.ncbi.nlm.nih.gov/pmc/articles/PMC4948226/*

[32] *https://link.springer.com/chapter/10.1007/978-3-319-60834-1_24*

[33] *https://en.wikipedia.org/wiki/Median_filter*

[34] *https://github.com/muthiyanbhushan/Image-Pre-processing-using-FPGA*

[35] *https://www.intechopen.com/books/medical-and-biological-image-analysis/active-contour-based-segmentation-techniques-for-medical-image-analysis*

[36] *Aggarwal, T., Furqan, A., & Kalra, K, "Feature extraction and LDA based classification of lung nodules in chest CT scan images", International Conference On Advances In Computing, Communications And Informatics (**2015**), DOI: 10.1109/ICACCI.2015.7275773.*

[37] *Jin, X., Zhang, Y. and Jin, Q, "Pulmonary Nodule Detection Based on CT Images Using Convolution Neural Network", 9Th International Symposium On Computational Intelligence And Design (**2016**), DOI: 10.1109/ISCID.2016.1053.*

[38] *Sangamithraa, P and Govindaraju, S, "Lung tumour detection and classification using EK-Mean clustering", International Conference On Wireless Communications, Signal Processing And Networking (**2016**). DOI: 10.1109/WiSPNET.2016.7566533.*

[39] *Roy, T., Sirohi, N., and Patle, A "Classification of lung image and nodule detection using fuzzy inference system", International Conference on Computing, Communication & Automation (**2015**), DOI: 10.1109/CCAA.2015.7148560.*

[40] *Ignatious, S and Joseph, R, "Computer aided lung cancer detection system", Global Conference On Communication Technologies (**2015**), DOI: 10.1109/GCCT.2015.7342723.*

[41] *Rendon-Gonzalez, E and Ponomaryov, V, "Automatic Lung nodule segmentation and classification in CT images based on SVM", 9Th International Kharkiv Symposium On Physics And Engineering Of Microwaves, Millimeter And Submillimeter Waves (**2016**). DOI: 10.1109/MSMW.2016.7537995.*

7. Acknowledgements:

We will give our sincere thanks to Kamaraj College of Engineering and Technology, Virudhunagar, India for doing this research work in the Department of Electronics and Communication Engineering. Our special thanks to Dr. Anant Achary, M.Tech., Ph.D., Principal, Kamaraj college of Engineering and Technology, Virudhunagar, India for his encouragement and continuous support for this research work. Our regards to Dr. Joe Pradeep Kumar, MBBS, Indian MRI Diagnostic & Research Limited, Madurai for his guidance and validation of data. The authors would like to thank all anonymous reviewers for their advice.